Competition between electromagnetically induced transparency and stimulated Raman scattering

Ken-ichi Harada, Tatsuya Kanbashi, and Masaharu Mitsunaga*
Graduate School of Science and Technology, Kumamoto University, Kumamoto 860-8555, Japan

Koji Motomura
Japan Science and Technology Agency, 4-1-8 Honmachi, Kawaguchi, 331-0012, Japan
(Received 30 September 2005; published 9 January 2006)

We claim that the concept of electromagnetically induced transparency is only valid for low atomic densities, and for high densities stimulated Raman scattering is totally dominant, where the incident probe wave is not transmitted but is converted to the Stokes wave. This behavior can be explained by the large difference in linear absorption coefficients between the probe and the Stokes waves. We have verified this claim by the experiments using sodium atomic vapor samples with and without a buffer gas. Theoretical analyses using the Liouville-Maxwell equations and numerical simulations also supported our observations.

DOI: 10.1103/PhysRevA.73.013807 PACS number(s): 42.65.Dr, 42.50.Gy

I. INTRODUCTION

Electromagnetically induced transparency (EIT) [1,2] is nowadays a quite established concept in the field of quantum optics and it has been applied to many topics such as precision spectroscopy including atomic clocks and magnetometers [3–5], ultraslow light [6], light storage [7–9], and quantum memory [10,11]. A typical EIT experiment is carried out by applying two resonant beams called probe beam (frequency ω_p) and coupling beam (frequency ω_c), to atoms having a Λ-type three-level system [see Fig. 1(a)] and detecting the probe beam transmission intensity, as shown in Fig. 1(b). A typical transmission spectrum is given in Fig. 1(c), featuring a sharp upward peak within the broad linear absorption, and the position of the sharp peak is determined by the two-photon resonance condition $\omega_0(\equiv\omega_p-\omega_c)=\omega_{21}$, where ω_{21} is the sublevel (hyperfine) splitting frequency of the medium. In interpreting this spectrum, it has long been considered that the medium becomes tranparent and the probe beam is going through it without attenuation. However, *is it really true?* In this paper we would like to warn that this spectrum does not necessarily mean EIT, but, instead, a Stokes wave with frequency $\omega_s\equiv 2\omega_c-\omega_p$ may be generated due to stimulated Raman scattering (SRS), which is enhanced by the two-photon resonance condition, $\omega_0=\omega_{21}$. Therefore, one can never judge from this spectrum if the sharp peak is attributed either to the transmitted probe wave (EIT) or to the newly generated Stokes wave (SRS), and the only way to nail down this controversy is to replace the detector by an optical spectrum analyzer, to frequency-decompose the output signal, and to check if the optical frequency is either ω_p (EIT), or ω_s (SRS).

Another viewpoint to attack this problem is as follows (see Fig. 2). Suppose that the probe and coupling beams prepared a coherent superposition state of the ground-state sublevels 1 and 2, or a dark state, which functions as a strong local oscillator with frequency ω_0. In this situation if the coupling wave with frequency ω_c once again comes into the system, there are two options to generate optical frequencies; either $\omega_c+\omega_0=\omega_p$ (EIT), or $\omega_c-\omega_0=\omega_s$ (SRS), as illustrated in Figs. 2(a) and 2(b). We need to consider which is the dominant process. At the first glance, one may think that EIT is favorable because it is a resonant process, while SRS is off-resonant and is much smaller by a factor of γ/ω_{21}, as shown in the theory section. (γ is the optical dephasing rate.) However, we have to take into account the propagation in the medium. Figure 2(c) shows linear absorption spectra of Na atoms and typical locations of ω_s, ω_c, ω_p, and ω_a ($\equiv 2\omega_p-\omega_c$: anti-Stokes frequency) with equal spacing ω_0. Ordinary EIT experiments are performed with probe frequency ω_p right at the peak of the absorption line, and the probe beam suffers from strong linear absorption as it propagates. Although the EIT effect exists, it cannot perfectly cancel out the overwhelming linear absorption. On the other hand, since ω_s is located away from the absorption center even including the Doppler broadening, it is free from attenuation. For example, when the atomic density is 3×10^{11} atoms/cm^3 and

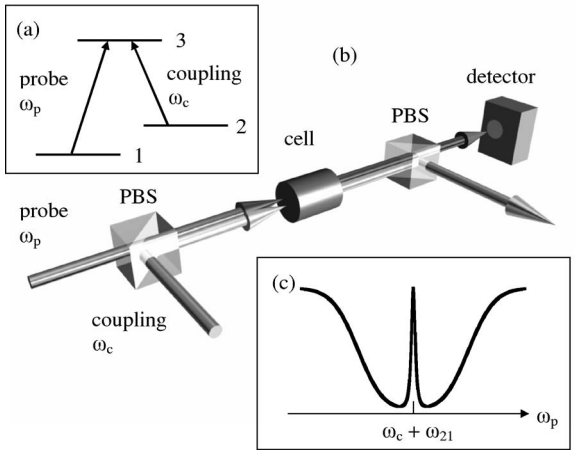

FIG. 1. (a) Λ-type three-level atoms with two incident fields, probe and coupling. (b) Schematic of a typical EIT experiment. PBS, polarizing beam splitter. (c) A typical EIT spectrum as a function of the probe frequency ω_p.

*Electronic address: mitunaga@sci.kumamoto-u.ac.jp

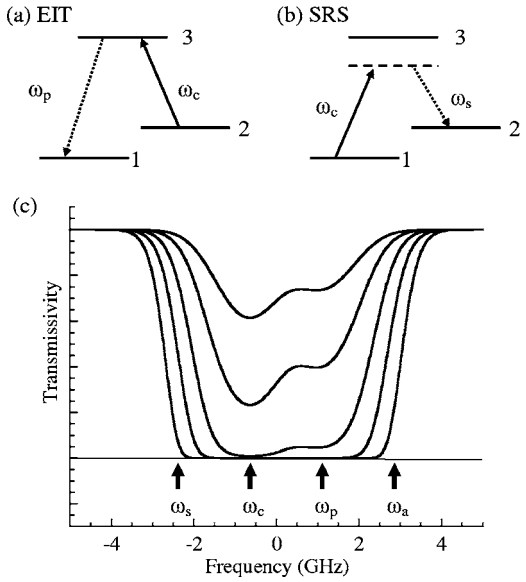

FIG. 2. (a) Three-level system displaying EIT. Incident coupling wave (ω_c) and the prepared sublevel coherence (ω_0) generate probe wave ($\omega_p=\omega_c+\omega_0$) causing EIT. (b) Three-level system displaying SRS. Incident coupling wave (ω_c) and the prepared sublevel coherence (ω_0) generate Stokes wave ($\omega_s=\omega_c-\omega_0$) causing SRS. (c) Doppler-broadened linear absorption spectra of Na atoms for atomic density of 1×10^{10}, 3×10^{10}, 1×10^{11}, 3×10^{11}, and 1×10^{12}atoms cm^{-3}. (From top to bottom. Sample length=8 cm.) Also shown are typical locations of ω_s, ω_c, ω_p, and ω_a with 1772 MHz spacing.

the sample length 8 cm, the transmissivity $T=0.6$ for Stokes, while 1×10^{-5} for probe; 60 000 times more favorable for the Stokes wave. In this way, we should not easily conclude that SRS is negligible compared to EIT.

The importance of SRS in analyzing EIT has been pointed out by a few workers [12,13], and frequency conversion [14,15], nondegenerate four-wave mixing [16,17], and sideband generation [18] using EIT have also been studied. Sideband generation using far-off-resonance Raman coherence has been reported [19,20]. However, no systematic study concerning competition between EIT and SRS in an ordinary EIT experiment has been carried out before.

In this paper we will experimentally show, by using sodium atomic vapor samples with and without a buffer gas, that the output signal in general is a mixture of EIT and SRS, and the EIT picture is only valid for low atomic densities and for high densities SRS is totally dominant. We will also develop a theoretical analysis for this observation by deriving coupled propagation equations for the probe and the Stokes beams and give some results of our numerical anaylses.

II. EXPERIMENT

We employed samples of sodium atomic vapor without a buffer gas and with a Ne buffer gas of several different pressures (1, 2, 5, 10, 30, and 100 Torr) to investigate this EIT vs SRS problem. Figure 3 shows our typical experimental setup [21–23]. A single-frequency ring dye laser (Coherent Radiation CR699-21) was tuned to the $3S_{1/2}-3P_{1/2}D_1$ transition of

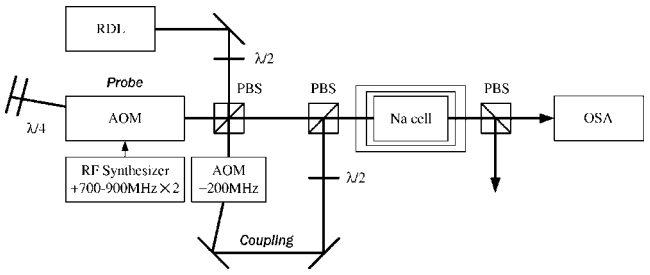

FIG. 3. Schematic of the experimental setup. RDL, ring dye laser; AOM, acousto-optic modulator; PBS, polarizing beam splitter; OSA, optical spectrum analyzer.

the Na atom at 589.6 nm and the output was divided into two for the probe beam and the coupling beam by the first polarizing beam splitter (PBS). The probe beam was frequency-scannable by using a double-pass acousto-optic modulator (AOM) driven by an RF synthesizer (+700 to 900 MHz driving frequency), while the coupling beam has a fixed frequency shift of −200 MHz. Consequently, the frequency difference $\omega_0\equiv\omega_p-\omega_c$ can be varied 1600 to 2000 MHz, covering the hyperfine splitting frequency $\omega_{21}=1772$ MHz of the Na atom. In this way we can easily set two-photon on-resonance ($\omega_0=\omega_{21}$) or off-resonance by the synthesizer tuning. The two-photon resonance linewidth was typically 400 kHz FWHM (full width at half maximum), much narrower than the Doppler width (~1.6 GHz) or the natural linewidth (10 MHz) of this transition. The powers of the probe and coupling beams were typically 3 mW and 12 mW, respectively, with spot sizes of about 2 mm. The probe and the coupling beams were recombined by the second PBS and were collinearly passed through a 7.5 cm long cell containing Na with magnetic shielding. Thus the probe and coupling polarizations were linear and orthogonal. In this type of lin ⊥ lin configuration, a simple symmetry consideration for the third-order nonlinear susceptibility shows that the output polarizations are such that probe and Stokes are horizontal, and coupling and anti-Stokes vertical. Therefore, by using the third PBS after the cell, we could pick up only the probe and the Stokes components and they were analyzed by an optical spectrum analyzer (OSA) with a free spectral range of 7.5 GHz. Every time an OSA output signal was obtained, a linear absorption spectrum for an extremely weak probe beam [24] was also measured in order to calculate the atomic densitiy using this data.

Typical OSA outputs are shown in Fig. 4, and they are critically dependent on if it is two-photon on-resonance ($\omega_0=\omega_{21}$) or off-resonance ($|\omega_0-\omega_{21}|>1$ MHz), and also on the atomic density (or, equivalently, the optical density) of the sample. (From now on the terms "on-resonance" and "off-resonance" refer to the two-photon resonance condition.) Figure 4(a) is the case of low atomic density ($N=3.5\times10^{10}$ cm^{-3} and peak linear transmission $T=40\%$), for off-resonance case and on-resonance case. The increase of transmission for the probe beam can be clearly seen when the on-resonance condition is satisfied, while the Stokes component is negligible. (Small peaks for the coupling components are leak signals due to the nonperfect PBS.) In this case the

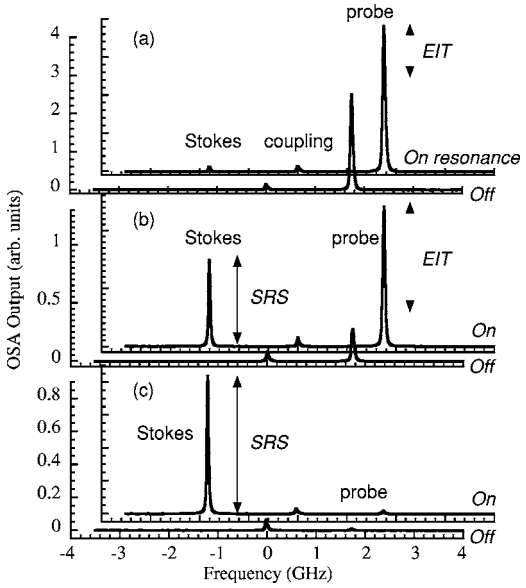

FIG. 4. OSA output spectra for the cases of two-photon on-resonance and off-resonance for three different atomic densities. (a) $N=3.5\times10^{10}$ cm^{-3} ($T=40\%$), (b) $N=1.2\times10^{11}$ cm^{-3} ($T=3\%$), and (c) $N=2.6\times10^{11}$ cm^{-3} ($T=0.06\%$). Three peaks in each figure correspond to probe, coupling, and Stokes components.

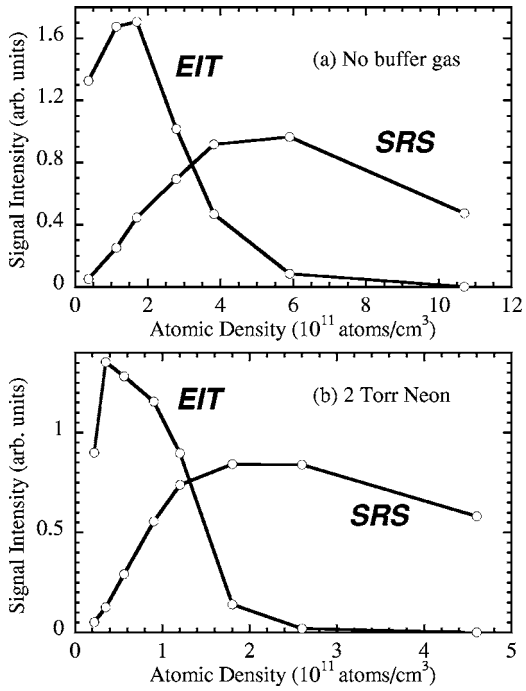

FIG. 5. EIT magnitude, S_{EIT}, and SRS magnitude, S_{SRS}, as a function of atomic denities for the samples with (a) no buffer gas and (b) 2 Torr Ne buffer gas. The solid lines are guidelines for the experimental data.

EIT interpretation is safely valid. In Fig. 4(b), when we increase the density up to $N=1.2\times10^{11}$ cm^{-3} ($T=3\%$), the on-resonance OSA output signal contains 50% probe component and 50% Stokes component, and in this case we are in a region of EIT-SRS mixture. When we go up further to the higher density region of $N=2.6\times10^{11}$ cm^{-3} ($T=0.06\%$), the probe component is zero even in the on-resonance condition, and the output signal is purely Stokes. Here the EIT picture breaks down and SRS is totally dominant.

Now let us define the EIT magnitude, S_{EIT}, as the difference between the on-resonance peak height and the off-resonance peak height of the probe component as indicated by the arrows in Fig. 4. Off course the SRS magnitude, S_{SRS}, is simply the height of the on-resonance Stokes component because the off-resonance Stokes component is always zero. Now we can plot S_{EIT} and S_{SRS} as a function of the atomic density, and the results are shown in Fig. 5 for the case of the sample without a buffer gas (a) and with a 2 Torr neon buffer gas (b). We have also performed the same experiments using cells with various buffer-gas pressures (1, 5, 10, 30 Torr) but the results are similar to the 2 Torr case. The curves for the no-buffer-gas case and the 2 Torr case also look very similar, and the tendency is, as we expected, for low density EIT is dominant and for high density SRS is dominant, although for the no-buffer-gas case it needs higher (by about a factor of 2) atomic density to generate SRS. The atomic density that gives equal amount of S_{EIT} and S_{SRS} is, then, about 3×10^{11} atoms/cm^3 for the no buffer gas case and about 1.5×10^{11} atoms/cm^3 for the 2 Torr buffer gas case.

In another experiment we checked the vertical polarization components including coupling and anti-Stokes, by analyzing the reflected beam by the output PBS. In this case, coupling and anti-Stokes replaced the roles of probe and Stokes, respectively, in the horizontal case, and gave exactly the same tendency. For low density, increase of the coupling transimission was dominant (EIT), but for high density anti-Stokes generation was dominant (SRS). Also in our previous report concerning the noncollinear diffraction type experiment called electromagnetically induced diffraction [23], where the diffraction spots were spatially separated as probe, coupling, Stokes, and anti-Stokes spots, we found that probe and coupling signals became null for high atomic densities, while Stokes and anti-Stokes signals remain strong. These findings once again confirm that the statement that the EIT picture is only valid for low densities is very universal.

III. THEORY

Now we found experimentally that SRS is crucially important in treating the EIT problem, we have to take into account, in addition to probe and coupling, all these sidebands (including higher order Stokes) with frequencies ω_s, ω_c, ω_p, ω_a, and so on in the theoretical analysis. The total electric field E_{total} should then be given as

$$E_{total} = \cdots + \mathcal{E}_s e^{-i\omega_s t} + \mathcal{E}_c e^{-i\omega_c t} + \mathcal{E}_p e^{-i\omega_p t} + \mathcal{E}_a e^{-i\omega_a t} + \cdots = \sum_j \mathcal{E}_j e^{-i\omega_j t}, \quad (1)$$

where the subscripts $j=\{\ldots,s,c,p,a,\ldots,\}$ denote {…, Stokes, coupling, probe, anti-Stokes, …}. In ordinary EIT-related theories these sidebands have been neglected and only two modes, ω_p and ω_c, have been treated, which of course resulted in no sideband generation. Besides, for the 1-to-3 transition the probe field has been assumed to be reso-

nant and the effect of coupling field has been neglected, while for the 2-to-3 transition it is the other way around. We now know that, in order to generate sidebands, these off-resonant fields play the important roles and these effects are treated rigorously. With this starting point, we solved the Liouville-Maxwell equations, and obtained the following coupled propagation equations for the probe amplitude $\mathcal{E}_p$ and the Stokes amplitude $\mathcal{E}_s$ [25,26]:

$$\frac{\partial \mathcal{E}_p}{\partial z} = -\frac{\alpha_p}{2}\mathcal{E}_p + c_{pp}|\mathcal{E}_c|^2\mathcal{E}_p + c_{ps}\mathcal{E}_c^2\mathcal{E}_s^*,$$

$$\frac{\partial \mathcal{E}_s}{\partial z} = -\frac{\alpha_s}{2}\mathcal{E}_s + c_{ss}|\mathcal{E}_c|^2\mathcal{E}_s + c_{sp}\mathcal{E}_c^2\mathcal{E}_p^*, \tag{2}$$

where $\alpha_j = kN/(\epsilon_0\hbar)(n_1|p_{31}|^2/\gamma_{j1} + n_2|p_{32}|^2/\gamma_{j2})$ $(j=\{p,s\})$ is the linear absorption coefficient for the probe or the Stokes wave. The four parameters are given as $c_{pp} = A\beta_1/\gamma_{p1}$, $c_{ps} = A\beta_2/\gamma_{p1}$, $c_{ss} = A\beta_2^*/\gamma_{s2}$, and $c_{sp} = A\beta_1^*/\gamma_{s2}$, where $A = kN|p_{31}|^2|p_{32}|^2/(2\epsilon_0\hbar^3)$, $\beta_1 = (n_1/\gamma_{p1} + n_2/\gamma_{c2}^*)/\gamma_0'$, and $\beta_2 = (n_1/\gamma_{c1} + n_2/\gamma_{s2}^*)/\gamma_0'$. k is wave vector, N is atomic density, $p_{3\ell}$ is dipole matrix element for the ℓ-to-3 transition. n_ℓ is the population of the level ℓ and $\gamma_{j\ell} = \gamma - i(\omega_j - \omega_{3\ell})$, where $j=\{p,c,s\}$ and $\ell=\{1,2\}$, and $\gamma_0' = \gamma_s + |\Omega_{c1}|^2/4\gamma_{s2}^* + |\Omega_{c2}|^2/4\gamma_{p1} - i(\omega_0 - \omega_{21})$, where $\Omega_{c\ell} = (2p_{3\ell}\mathcal{E}_c)/\hbar$ is the Rabi frequency for the coupling beam. γ and γ_s are the dephasing rates for the optical transitions and the sublevel transition. For an inhomogeneous broadening case, the parameters should be averaged over the Doppler profile.

In this derivation we adopted the same assumption as the ordinary EIT theory, that is, that the coupling field is much stronger than the probe field, and the probe field (and consequently the sidebands) is treated perturbatively. The coupling beam is, therefore, not affected by the probe or the Stokes beam, although it may attenuate by its own linear and nonlinear absorption.

The interpretation of each term in Eq. (2) is very simple and clear. The first terms of the equations describe linear absorption (LA), since these exist even without coupling field $\mathcal{E}_c$, and the fields decay exponentially with their own absorption coefficients α_p and α_s. The second terms are EIT terms and the absorption of each wave is reduced with the help of $\mathcal{E}_c$. It is also easily shown that, the effective absorption coefficients $\alpha_p - 2c_{pp}|\mathcal{E}_c|^2$ is equal to the well-known EIT absorption coefficient. This indicates that our theory is readily reduced to the ordinary EIT theory if the Stokes field is neglected. Finally, the third terms show SRS and the probe and the Stokes interact with each other through these terms.

The most trivial case is the case of no coupling beam ($\mathcal{E}_c = 0$) or two-photon off-resonance ($|\omega_0 - \omega_{21}| \gg |\Omega_c|^2/\gamma$). In this case it is easily shown that the above coupled equations are decoupled and only the first terms remain, and the probe wave and the Stokes wave exponentially attenuate independently according to α_p and α_s.

To extract the essential parts of the equations, we will make several assumptions: (1) homogeneous broadening, (2) one-photon resonant ($\omega_p = \omega_{31}$ and $\omega_c = \omega_{32}$), (3) two-photon resonant ($\omega_0 = \omega_{21}$), (4) large hyperfine splitting compared to the optical dephasing rate ($\omega_{21} \gg \gamma$) and (5) population accumulated in level 1 ($n_1 = 1$ and $n_2 = 0$). Although the first assumption is against our experimental situation, all the others are reasonable. Under these conditions, the above equations can become quite simple, making all the quantities real, and written as

$$\frac{\partial \mathcal{E}_p}{\partial z} = -\frac{\alpha_0}{2}\mathcal{E}_p + \frac{\alpha_0}{2}\eta_c\mathcal{E}_p - \frac{\alpha_0}{2}\eta_c\frac{\gamma}{\omega_0}\mathcal{E}_s',$$

$$\frac{\partial \mathcal{E}_s'}{\partial z} = -\frac{\alpha_0}{2}\left(\frac{\gamma}{2\omega_0}\right)^2\mathcal{E}_s' + \frac{\alpha_0}{2}\eta_c\left(\frac{\gamma}{\omega_0}\right)^2\mathcal{E}_s' - \frac{\alpha_0}{2}\eta_c\frac{\gamma}{\omega_0}\mathcal{E}_p, \tag{3}$$

where $\mathcal{E}_s' = i\mathcal{E}_s^*$ and $\alpha_0 = kN|p_{31}|^2/(\epsilon_0\hbar\gamma)$ is the peak linear absorption coefficient and

$$\eta_c = \frac{|\Omega_{c2}|^2/4\gamma\gamma_s}{1 + |\Omega_{c2}|^2/4\gamma\gamma_s}, \tag{4}$$

is the saturation parameter and varies from zero (no coupling case) to 1 (strong coupling regime). Remember that the saturation factor $|\Omega_{c2}|^2/4\gamma\gamma_s$ is given by the ratio of the optical pumping rate $|\Omega_{c2}|^2/4\gamma$ and the sublevel dephasing rate γ_s and this saturation intensity is much smaller than what is needed to saturate the optical transition. In Eq. (3) all the terms are classified by the order of (γ/ω_0). The LA and EIT of probe are of the same order. Both the SRS terms for the probe and coupling are of the order of (γ/ω_0) and their magnitudes are smaller by this factor. The LA and EIT terms of Stokes are even smaller, of the order of $(\gamma/\omega_0)^2$.

The above simplified coupled equations can be numerically solved with the boundary conditions of $\mathcal{E}_p(0) = \mathcal{E}_0$ and $\mathcal{E}_s'(0) = 0$. Figure 6 shows the results of the numerical simulation for three different absorption coefficients (a) $\alpha_0 = 0.2\ \mathrm{cm}^{-1}$, (b) $\alpha_0 = 0.7\ \mathrm{cm}^{-1}$, and (c) $\alpha_0 = 1.2\ \mathrm{cm}^{-1}$. With the sample length $\ell = 8$ cm, the linear transmissivity $T = \exp[-\alpha_0\ell] =$ (a)0.20, (b) 3.7×10^{-3}, and (c) 6.8×10^{-5}. (In this simulation the attenuation of the coupling beam was also taken into account.) The three curves in each figure show the propagation behaviors of probe intensity with two-photon off-resonance (probe, LA), probe intensity with two-photon on-resonance (probe, EIT), and Stokes intensity with two-photon on-resonance (Stokes). As we expected, for low optical density (a), the phenomenon can be well interpreted in terms of EIT and the resonance enhancement of the probe beam is very pronounced, while Stokes component is rather negligible. For middle density (b), the probe and the Stokes contributions are nearly equal. For high density (c), the probe component is totally negligible due to strong linear absorption. Once the probe energy is converted to Stokes, however, it can go through the medium without attenuation all the way up to the end of the cell.

A numerical simulation for the density (or, equivalently, absorption coefficient) dependence of the EIT and SRS magnitudes, S_{EIT} and S_{SRS}, as defined in the experiment section, is shown in Fig. 7 and the overall behavior is quite similar to the observations (Fig. 5), reconfirming our main conclusion, that is, EIT (SRS) is dominant for low (high) density. Note that the Stokes intensity remains almost constant for high atomic densities, and the probe power is either dissipated in

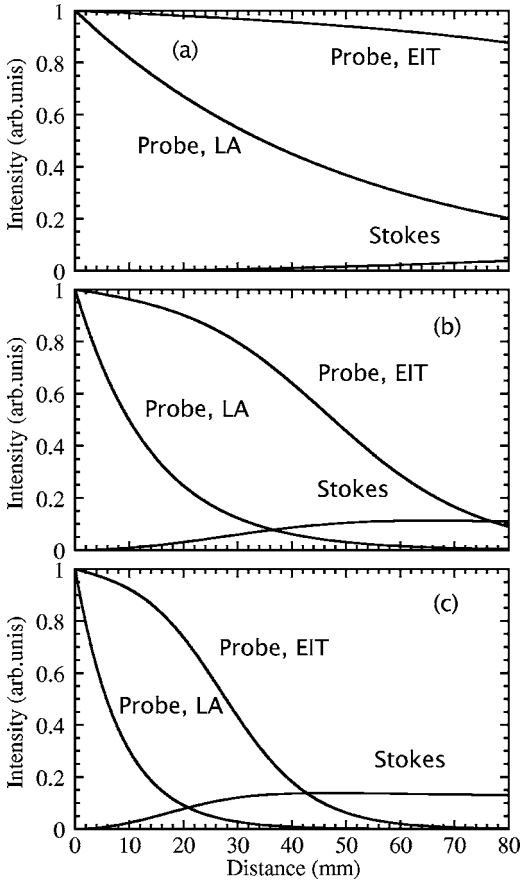

FIG. 6. Numerical simulation of the beam intensities as a function of propagation distance in the medium for three different absorption coefficients α_0: (a) $\alpha_0=0.2$ cm^{-1}, (b) $\alpha_0=0.7$ cm^{-1}, and (c) $\alpha_0=1.2$ cm^{-1}. (Probe, LA), probe intensity $\mathcal{E}_p^2(z)$ for two-photon off-resonance showing linear absorption. (Probe, EIT), probe intensity $\mathcal{E}_p^2(z)$ for two-photon on-resonance showing the EIT enhancement. (Stokes), Stokes intensity $\mathcal{E}_s'^2(z)$ for two-photon on-resonance showing SRS. Attenuation of the coupling beam was taken into account.

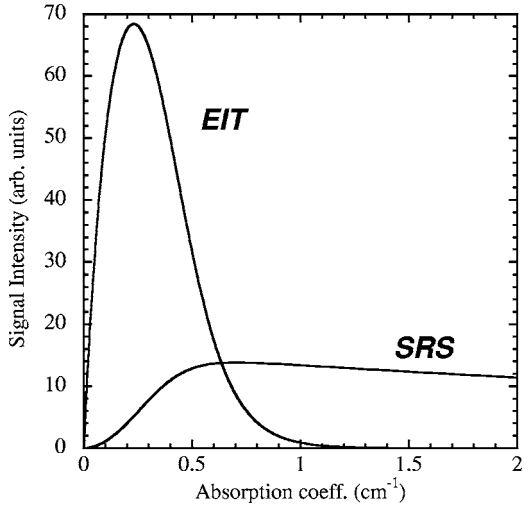

FIG. 7. Numerical simulation of EIT magnitude, S_{EIT}, and SRS magnitude, S_{SRS}, as a function of the absorption coefficient α_0. The sample length is 8 cm.

the medium or converted to the Stokes wave with a certain ratio. One question arises as to whether the number density at which SRS becomes dominant depends on the coupling intensity or not. Experimentally we have not checked this point, but numerically we have found that it is almost constant for a wide range of coupling intensities, because, if the coupling intensity is increased, both EIT and SRS are increased likewise.

IV. DISCUSSION AND CONCLUSION

Through the experimental observations and theoretical analyses, we have confirmed that, in ordinary EIT experiments, the so-called EIT picture is only valid for low optical densities, and for high densities the output signal is 100% converted from the probe wave to the Stokes wave. There have been a tremendous amount of EIT-related papers published so far, but in some of them what they believed they observed as EIT may have been SRS. From this viewpoint it should be definitely worthwhile to double check all the previous EIT-related topics. For example, how about the precision spectroscopy including atomic clocks and magnetometers? We believe that this topic should not be modified even with the existence of the Stokes waves, since the resonance behaviors of the EIT term and the SRS term are exactly the same, as shown in Eq. (2), and so the precision should remain the same. How about ultraslow light problem? Here, the inclusion of the Stokes wave may complicate the problem because the group velocity of the Stokes wave may not be the same as that of the probe wave, and thus the probe and the Stokes waves may not copropagate in the medium. This problem should be studied further. And, finally, how about the light storage problem? We can store the optical information in the sublevel coherence by applying the probe pulse and the coupling pulse. The problem is that, when the readout pulse is applied, we will not know whether the output signal is either the probe wave or the Stokes wave. The situation should remain the same for quantum optical information and we will not know if it is a probe photon or a Stokes photon. Our preliminary light-storage experiment once again indicated that, the frequency of the readout signal depended on the atomic density, and for low densities it was ω_p but for high densities it was ω_s. This light storage problem should definitely be investigated in detail and that is what we are going to challenge in the next stage.

[1] K.-J. Boller, A. Imamoğlu, and S. E. Harris, Phys. Rev. Lett. **66**, 2593 (1991).
[2] J. E. Field, K. H. Hahn, and S. E. Harris, Phys. Rev. Lett. **67**, 3062 (1991).
[3] R. Wynands and A. Nagel, Appl. Phys. B: Lasers Opt. **68**, 1 (1999).
[4] M. Merimaa, T. Lindvall, I. Tittonenm, and E. Ikonen, J. Opt. Soc. Am. B **20**, 273 (2003).
[5] H. Asahi, K. Motomura, K. Harada, and M. Mitsunaga, Opt. Lett. **28**, 1153 (2003).
[6] L. V. Hau, S. E. Harris, Z. Dutton, and C. H. Behroozi, Nature (London) **397**, 594 (1999).
[7] M. Fleischhauer and M. D. Lukin, Phys. Rev. Lett. **84**, 5094 (2000).
[8] C. Liu, Z. Dutton, C. H. Behroozi, and L. V. Hau, Nature (London) **409**, 490 (2001).
[9] D. F. Phillips, A. Fleischhauer, A. Mair, R. L. Walsworth, and M. D. Lukin, Phys. Rev. Lett. **86**, 783 (2001).
[10] M. D. Lukin, A. B. Matsko, M. Fleischhauer, and M. O. Scully, Phys. Rev. Lett. **82**, 1847 (1999).
[11] C. H. van der Wal, M. D. Eisaman, A. André, R. L. Walsworth, D. F. Phillips, A. S. Zibrov, and M. D. Lukin, Science **301**, 196 (2003).
[12] M. M. Kash, V. A. Sautenkov, A. S. Zibrov, L. Hollberg, G. R. Welch, M. D. Lukin, Y. Rostovtsev, E. S. Fry, and M. O. Scully, Phys. Rev. Lett. **82**, 5229 (1999).
[13] V. Wong, R. S. Bennink, A. M. Marino, R. W. Boyd, C. R. Stroud, Jr., and F. A. Narducci, Phys. Rev. A **70**, 053811 (2004).
[14] M. Jain, H. Xia, G. Y. Yin, A. J. Merriam, and S. E. Harris, Phys. Rev. Lett. **77**, 4326 (1996).
[15] A. J. Merriam, S. J. Sharpe, M. Shverdin, D. Manuszak, G. Y. Yin, and S. E. Harris, Phys. Rev. Lett. **84**, 5308 (2000).
[16] P. R. Hemmer, D. P. Katz, J. Donoghue, M. Cronin-Golomb, M. S. Shahriar, and P. Kumar, Opt. Lett. **20**, 982 (1995).
[17] B. Lü, W. H. Burkett, and M. Xiao, Opt. Lett. **23**, 804 (1998).
[18] A. F. Huss, N. Peer, R. Lammeggar, E. A. Korsunsky, and L. Windholz, Phys. Rev. A **63**, 013802 (2000).
[19] K. Hakuta, M. Suzuki, M. Katsuragawa, and J. Z. Li, Phys. Rev. Lett. **79**, 209 (1997).
[20] J. Q. Liang, M. Katsuragawa, F. Le Kien, and K. Hakuta, Phys. Rev. Lett. **85**, 2474 (2000).
[21] K. Motomura, T. Koshimizu, K. Harada, H. Ueno, and M. Mitsunaga, Opt. Lett. **29**, 1141 (2004).
[22] K. Harada, K. Motomura, T. Koshimizu, H. Ueno, and M. Mitsunaga, J. Opt. Soc. Am. B **22**, 1105 (2005).
[23] K. Harada, S. Tanaka, T. Kanbashi, M. Mitsunaga, and K. Motomura, Opt. Lett. **30**, 2004 (2005).
[24] R. Walkup, A. Spielfiedel, W. D. Phillips, and D. E. Pritchard, Phys. Rev. A **23**, 1869 (1981).
[25] M. D. Lukin, M. Fleischhauer, A. S. Zibrov, H. G. Robinson, V. L. Velichansky, L. Hollberg, and M. O. Scully, Phys. Rev. Lett. **79**, 2959 (1997).
[26] M. D. Lukin, P. R. Hemmer, M. Löffler, and M. O. Scully, Phys. Rev. Lett. **81**, 2675 (1998).